View metadata, citation and similar papers at core.ac.uk

brought to you by CORE

provided by Elsevier - Publisher Connector

Available online at www.sciencedirect.com

ScienceDirect

Procedia Computer Science 4 (2011) 1135–1144

Procedia Computer Science

International Conference on Computational Science, ICCS 2011

An ab initio study of Xe–NO($X^2\Pi$) and Xe–NO($A^2\Sigma^+$) potential energy surfaces

Juan Carlos Castro-Palacio[a,*], Keisaku Ishii[b], Jesús Rubayo-Soneira[c], Koichi Yamashita[b,*]

[a]*Departamento de Física, Universidad de Pinar del Río. Martí 270, Esq. 27 de Noviembre, Pinar del Río, CP-20100 Cuba*
[b]*Department of Chemical System Engineering. Graduate School of Engineering. The University of Tokyo,Tokyo 113-8656, Japan.*
[c]*Departamento de Física General y Matemáticas. Instituto Superior de Tecnologías y Ciencias Aplicadas, Quinta de los Molinos, Ave. Carlos III y Luaces, Plaza C. Habana, Cuba*

Abstract

The potential energy surfaces (PESs) of Xe–NO($X^2\Pi$) and Xe–NO($A^2\Sigma^+$) complexes have been obtained using highly accurate ab initio calculations. Analytical representations of these PESs were obtained using a Legendre polynomial interpolation. In the ground state, the surfaces A′ and A″ show two linear wells at short distances (4.0–4.5 Å) with energies between –67 and –135 cm^{-1}. The surface A′, unlike that of A″, presents a T-shape well at –85 cm^{-1}. To evaluate the influence of corrections for quadruple excitations on the topology of the Xe–NO($A^2\Sigma^+$) PES, calculations were performed with and without considering corrections for quadruple excitations. Both surfaces present two linear wells between 4.9 and 6.8 Å but when considering corrections for quadruple excitations the wells are more than twice as deep (–64 and –40 cm^{-1}) as when not considering these corrections (–25 and –20 cm^{-1}).

Keywords: ab initio potential energy surface, Xe-NO, electronic ground ans excited states

1. Introduction

Although many experimental studies related to molecules trapped in Xe matrices and clusters are available [1–15], little theory has been published [16–20], even with the current development of density functional theory methods and the increasing power of computers [21,22]. In this respect, the possibility of producing interaction potential energy surfaces (PESs) allows the performance of classical molecular dynamics simulations, which represent a very valuable tool and most times the sole way for dealing with large systems. On the other hand, the present pool of experimental data is still insufficient for the complete characterization of many phenomena occurring on the atomic scale. The latter is the case for photoinduced processes consisting of cage relaxation upon

1877–0509 © 2011 Published by Elsevier Ltd. Open access under CC BY-NC-ND license.
Selection and/or peer-review under responsibility of Prof. Mitsuhisa Sato and Prof. Satoshi Matsuoka
doi:10.1016/j.procs.2011.04.121

Rydberg excitation of impurities in rare gas (RG) solids [23–30], such as (NO, Hg, I_2)-doped RG solids [24,25,29,31] and H_2 solids [24,27,30,32,33].

The response in these systems upon a low-*n* Rydberg photoexcitation of an active center is followed by an induced intramolecular motion and consequent nuclear dynamics of the surrounding cage [34–36] with long-range propagation of energy [36–38]. Consequently, a large blue spectral shift in absorption is observed compared with the gas phase, which is connected to the strong short-range repulsion between the Rydberg electron and the closed shell of the RG atoms [23,25]. This strong repulsion is responsible for configurational rearrangements of the cage species surrounding the excited center leading to a new equilibrium configuration from which fluorescence takes place. The large absorption–emission Stokes shifts that are observed reveal the extensive configurational changes around the excited species. The basic mechanism is considered to be a radial expansion of the cage (the so-called electronic "bubble" formation) [23,25,26,39] that is also operative in RG liquids and clusters [23,39,40].

In this respect, classical molecular dynamics simulations have been carried out to describe the dynamics of structural relaxation and energy redistribution in these systems, such as the dynamics of structural relaxation in NO-doped Ne, Ar, Kr and Xe solids upon Rydberg photoexcitation of the impurity [17,41–46]. These studies have used isotropic potentials for the NO($X^2\Pi$)–RG interactions from the experimental results of Thuis *et al.* [47] for RG = Ar, Kr, Xe and from reference [48] for RG = Ne. However, for the NO($A^2\Sigma^+$)–RG (RG = Ne, Kr, Xe) interactions, several theoretical approaches have been used. To model NO($A^2\Sigma^+$)–Ne interactions in solid Ne, a Born–Mayer potential obtained from a semiclassical projection method has been used [42,43]. In the case of modeling NO($A^2\Sigma^+$)–Kr, Xe interactions, both Lennard-Jones and Born–Mayer potentials have been fitted to the experimental spectroscopic data available for these systems. A common point in these studies was the use of isotropic PESs, where the angular dependence has been neglected under certain conditions.

In references [49–51], ab initio PESs were used to study the structural dynamics of NO-doped Kr solid so that the angular variation of potential was considered. Results for this last system showed that the curve of the isotropic ab initio potential (first term in the expansion of the PES in Legendre polynomials) in the ground state (Kr–NO($X^2\Pi$)) almost overlaps the semiempirical potential of Thuis *et al.* [47], showing that the anisotropy is unimportant. However, in the case of the excited state (Kr–NO($A^2\Sigma^+$)) some differences were noticed in the dynamics when the isotropic ab initio potential and the fitted potentials for Kr–NO($A^2\Sigma^+$) in reference [45] were used, indicating that the anisotropy of potentials and the many-body effects play a role. In the calculation of the Kr–NO($A^2\Sigma^+$) PES, corrections for quadruple excitations were not taken into account. However, because the consideration of these corrections causes some changes in the topology of the PESs, changes in the dynamics would be expected.

In this work, PESs for Xe–NO($X^2\Pi$) and Xe–NO($A^2\Sigma^+$) complexes calculated using ab initio calculations are presented. The availability of these PESs allows more complete simulations of the dynamics of structural relaxation of the NO-doped Xe system upon photoexcitation of the impurity. Results for these simulations are compared with those obtained in reference [17], where isotropic potentials were used and to the available experimental data, namely, the spectroscopic results for the $X^2\Pi \rightarrow A^2\Sigma^+$ transition of NO in rare gas solids by Chergui *et al.* [25]. These PESs will also be valuable for dynamic studies involving the Xe–NO triatomic system. As these simulations use pair additivity in the potentials, an important issue is to evaluate the influence of nonadditive effects for this type of system and the highly polarizable nature of the A state.

The outline of the paper is as follows. In section II we show the methodology for the ab initio techniques used in the calculations and for the fitting of the analytical PES. In section III we present the results and discussion in comparison with similar published results and finally some conclusions are drawn in section IV.

2. Methodology

The spin-restricted coupled cluster (RCCSD(T)) method [63] has been used for the calculations in the ground $1^2A'$ (NO($A^2\Sigma^+$)–Xe) state and the complete active space self-consistent field (CASSCF) [52] and the multireference singles and doubles internally contracted configuration interaction (MRCI) [53] method for the excited $2^2A'$ (NO($A^2\Sigma^+$)–Xe) state. Jacobi-coordinates were employed (*r*: the NO bond length, *R*: the distance between the center of mass of NO and the Xe atom, α: the Jacobi angle, 0º corresponds to the linear Xe–NO and 180º to the linear Xe–ON, respectively). In the RCCSD(T) calculations for the $1^2A'$ state, *r* was fixed at 1.15 Å, which is the equilibrium bond length of the $X^2\Pi$ state of the diatomic NO molecule. The basis set superposition error (BSSE) was corrected using Boys and Bernardi's counterpoise procedure in the RCCSD(T) calculations. The $1^2A'$, $1^2A''$, and $2^2A'$ states

were averaged with equal weights and r was fixed at 1.06 Å, which is the equilibrium bond length of the $A^2\Sigma^+$ state of NO. The valence 16a′–21a′ and 6a″–7a″ orbitals, corresponding to the 3σ–6σ and 1π–2π orbitals of the diatomic NO, and one 3s-Rydberg orbital (a′ symmetry) were included in the active space. In the MRCI calculations, valence 18a′–20a′ and 6a″–7a″ orbitals and one 3s-Rydberg orbital were employed for the reference space. As to the basis functions, Hirao groups VTZ to include relativistic corrections and the 3rd-order Douglas–Kroll–Hess transformation [54,55] were used. For N and O, three s-type and three p-type diffuse functions, generated as even-tempered functions, were augmented to describe a 3s-Rydberg electron for the $2^2A'$ state (NO($A^2\Sigma^+$)–Xe). The energies were calculated at 155 points in the range $2.5 \leq R \leq 20.0$ Å and at α = 0º, 45º, 90º, 135º, 180º. All calculations were carried out using the MOLPRO program [56]. For nonsize-extensive approaches, such as MRCI, the application of the standard Boys–Bernardi counterpoise correction leads to meaningless results, even if standard size-consistency Davidson's corrections are considered. This aspect is discussed in detail in references [56–62].

To represent the two-dimensional interaction potentials for the NO($A^2\Sigma^+$)–Xe triatomic system we used an expansion in Legendre polynomials to fit the CASSCF–MRCI ab initio data,

$$V(R,\alpha) = \sum_{k=0}^{N} f_k(R) P_k(\cos\alpha), \tag{1}$$

where $f_k(R)$ are the radial coefficients.

By making an expansion up to order N (number of ab initio points for the R_j coordinates at each α_i direction) for M values of the Jacobi angle we can write down an $M \times N$ linear system, from which the values of the coefficients $f_k(R)$ are obtained. Taking into account that potential energy values do not change significantly with variations of the Jacobi angle, it is reliable to use only a few terms of the expansion to fit the ab initio data. Our expansion includes five terms (the same number of angular directions used in the ab initio calculations) so that we can solve a compatible linear system. Radial coefficients were obtained by an interpolation using splines allowing the final representation of the PES. All calculations were performed using Fortran code written by the authors.

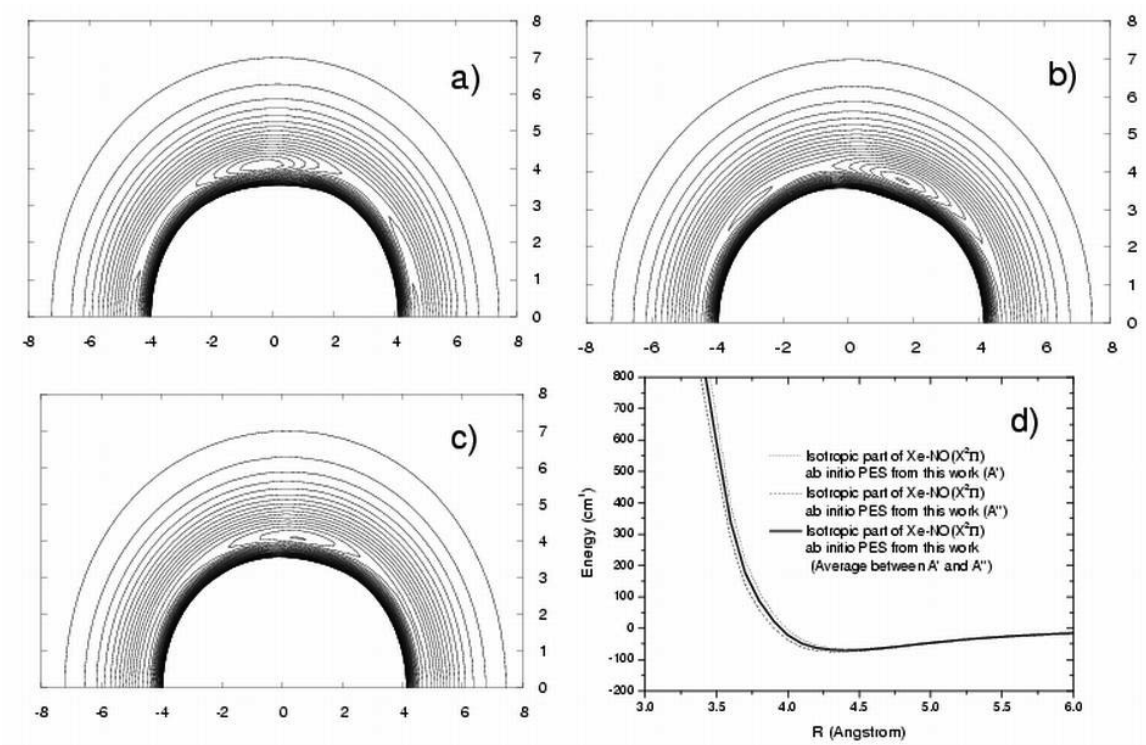

Fig. 1. Contour plots of the NO($X^2\Pi$)–Xe PES. Contour intervals are at 5 cm^{-1} and for energies from –200 to 100 cm^{-1}. The N–O distance is fixed at r = 1.15 Å for all calculations. The A′ PES is represented in panel a, A″ PES in panel b, the average (A′ + A″)/2 in panel c and the isotropic parts of A′ and A″ in panel d.

3. Results and discussion

Two-dimensional contour plots of the $V(R, \alpha)$ surface for the NO($X^2\Pi$)–Xe triatomic system in the XY-plane are presented in Figure 1. The A′ PES (panel a) presents two linear wells at 4.7 Å ($\alpha = 0º$) and 4.5 Å ($\alpha = 180º$) with energies of –70 cm^{-1} and –70 cm^{-1}, respectively; and a T-shape well at 4.0 Å ($\alpha = 95º$), which is –85 cm^{-1} deep. The A″ PES (panel b) presents only two wells at 4.17 Å ($\alpha = 130º$) and 3.81 Å ($\alpha = 79º$) with energies of –90 cm^{-1} and –85 cm^{-1}, respectively. However, the average PES ((A′ + A″)/2) (panel c) has only a well at 4.0 Å ($\alpha = 83º$), which is –85 cm^{-1} deep. The isotropic parts of A′, A″ and average PESs (when PESs are expanded in Legendre polynomials) are shown in panel d. The results indicate that the isotropic curves for A′ and A″ are very similar and so is the isotropic part for the average PESs. This fact demonstrates that the differences between the isotropic curves for A′ and A″ correspond to the anisotropic terms in the series expansion.

Two-dimensional contour plots of the $V(R, \alpha)$ surface for the NO($A^2\Sigma^+$)–Xe triatomic system in the XY-plane are presented in Figure 2. The PES that includes corrections for quadruple excitations (panel a) shows only two linear wells at 4.9 Å ($\alpha = 0º$) and 6.2 Å ($\alpha = 180º$) with energies of –64 cm^{-1} and –40 cm^{-1}, respectively. The PES that does not include corrections for quadruple excitations (panel b) also shows only two linear wells at 6.0 Å ($\alpha = 0º$) and 6.8 Å ($\alpha = 180º$) with energies of –25 cm^{-1} and –20 cm^{-1}, respectively. The isotropic parts of the PESs in panels a and b are shown in panel c. The results indicate that when corrections for quadruple excitations are taken into consideration the potential is less repulsive and less energetic when compared with the case where they are not considered. However, for distances beyond 8.0 Å both curves show isotropic behavior. The isotropic parts for the ground (average curve) and excited state (including quadruple excitations) are shown in panel d. The gap between the ground state and the first Rydberg state has been omitted in the picture.

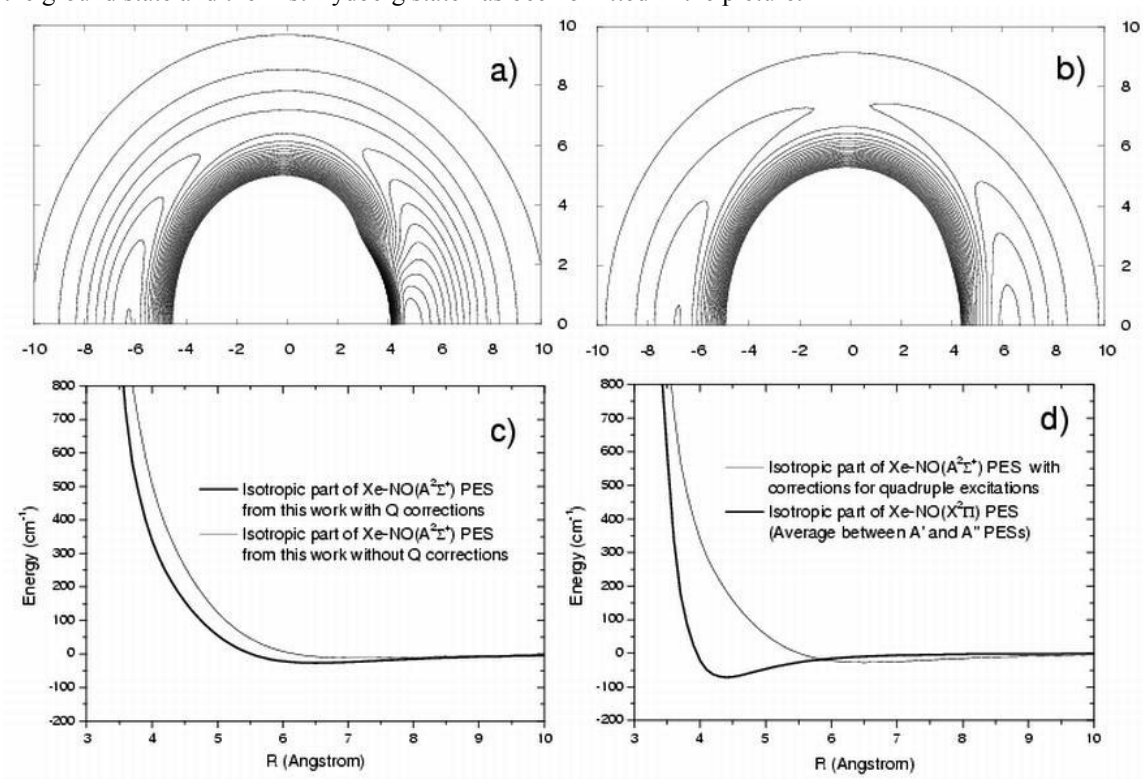

Fig. 2. Contour plots of the NO($A^2\Sigma^+$)–Xe PES. Contour intervals are at 5 cm^{-1} and for energies from –200 to 100 cm^{-1}. The N–O distance is fixed at r = 1.06 Å for all calculations. Panel a shows the case when corrections for the quadruple excitations are considered, and panel b when they are not. Panel c shows the isotropic parts of PESs from panels a and b. Panel d shows the isotropic parts of the NO($X^2\Pi$)–Xe PES (average (A′ + A″)/2) and the NO($A^2\Sigma^+$)–Xe PES (with quadruple excitations).

The radial coefficients in eq. 1 are shown in Figure 3 versus the distance for the ground (panel a) and excited state (panel b). It can be seen that the isotropic term (f_0) dominates the expansion for both cases. The terms f_1, f_3 and f_4 represent small contributions while f_2 contributes appreciably. In the case of the excited state, the term f_1 hardly contributes, terms f_3 and f_4 contribute mildly and f_2 very noticeably even for the well part. The nonnegligible contributions of higher order terms indicate that the radial contribution of the anisotropic terms should be taken into account to properly represent the radial dependence of the potential. At the same time, it means that the higher order terms in the series are important for the topology of the PES. For distances beyond 5.0 Å all terms converge, only the first term remaining important.

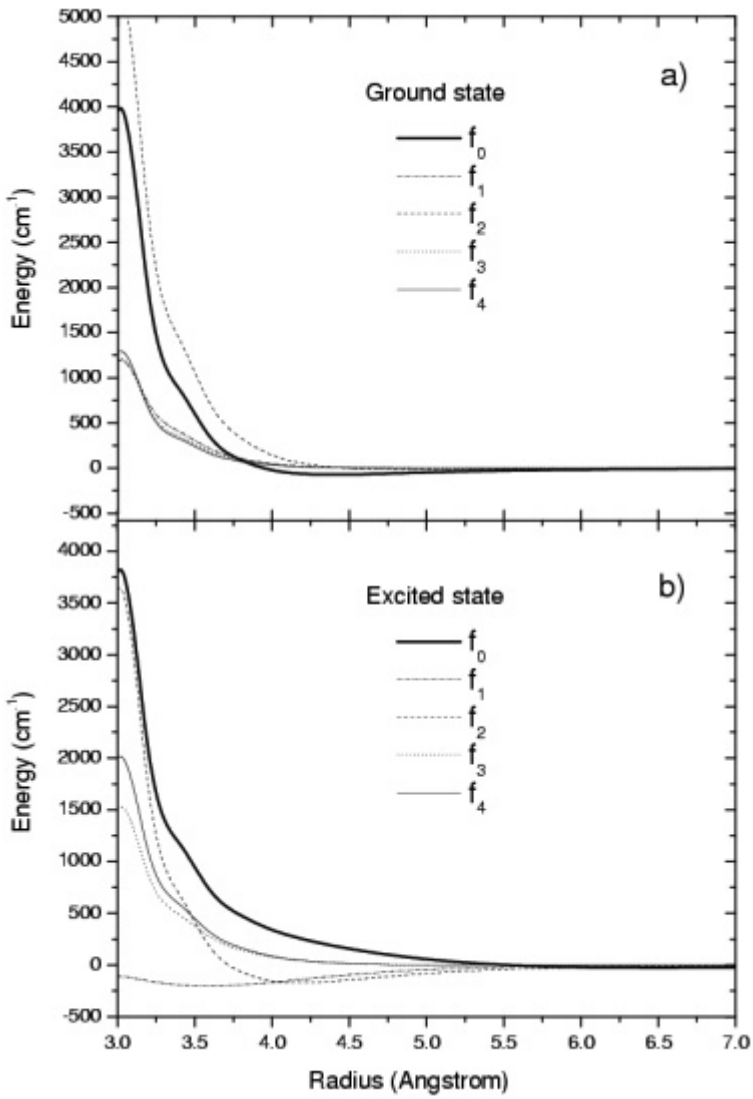

Fig. 3. Radial coefficients ($f_0, f_1, \ldots, f_4$) of the interaction potential versus the intermolecular distance, when expanded in Legendre polynomials. Results for the NO($X^2\Pi$)–Xe PES are shown in panel a, while results for the NO($A^2\Sigma^+$)–Xe PES including corrections for quadruple excitations are shown in panel b.

The sums of the expansion terms up to the first, second, third, fourth and fifth terms (F_0, F_1, ... , F_4, respectively) are plotted in Figure 4 for $\alpha = 0º$, 45º, 90º and 180º directions of the NO($A^2\Sigma^+$)–Xe PES. For $\alpha = 90º$ (T-shape) and

$\alpha = 180^{\circ}$ (linear shape) there is a very good convergence because only two terms are necessary; however, for $\alpha = 0^{\circ}$ (linear) and $\alpha = 45^{\circ}$ all five terms of the expansion should be included. In this last case convergence could be improved if more terms were to be taken, which is equivalent to saying that more ab initio points would be needed. Even so, we believe that this lack of total convergence will not lead to appreciable changes in the results of the upcoming molecular dynamic simulations on NO-doped Xe solids (currently underway). The inclusion of all terms in the expansion of the PES allows a proper representation of the short-range part of the potential, where the Franck–Condon region for NO-doped Rydberg excitation is located, because of the importance of the angular contributions to the potential. For distances beyond 5.0 Å, the first term is enough to represent the PES, because there is a full coincidence of all terms (isotropic region).

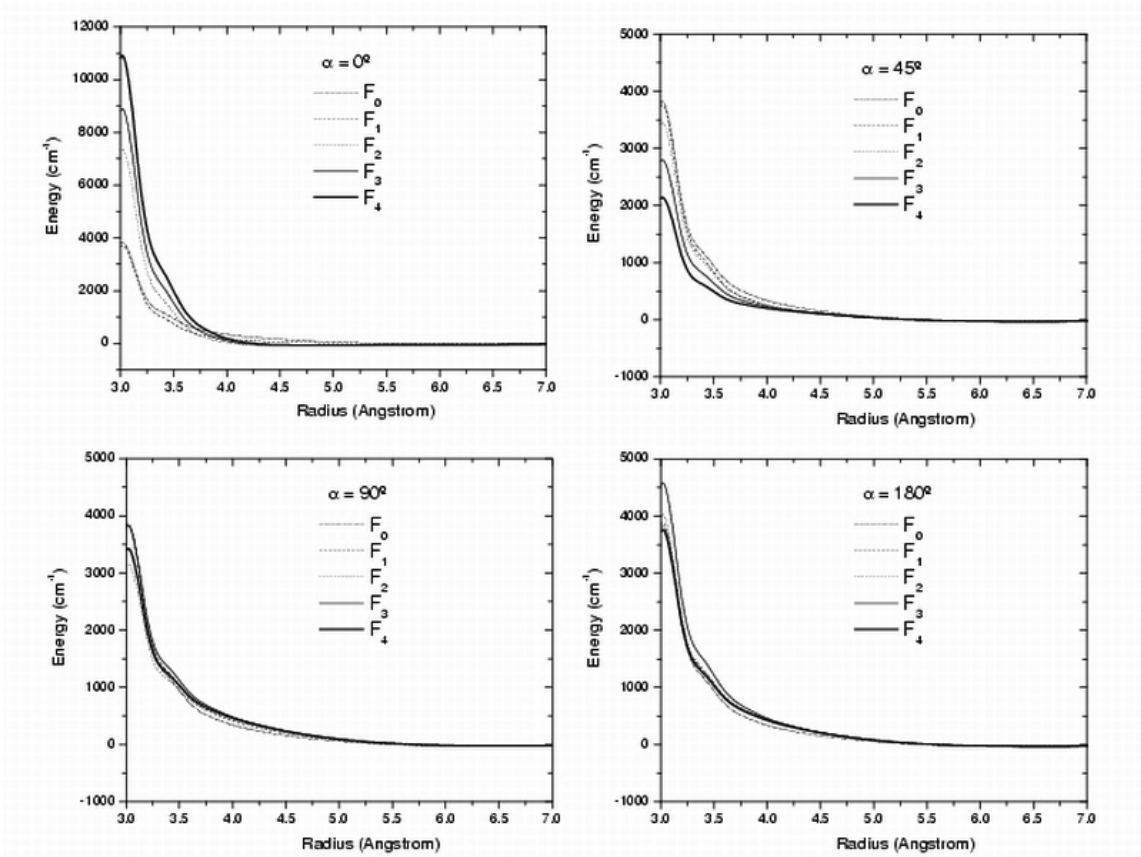

Fig. 4. Coefficients (whole term) of the interaction potential versus the intermolecular distance, when expanded in Legendre polynomials. The variables F_0, F_1, ... , F_4 indicate the total sum up to the first, second, third, fourth and fifth term, respectively. Results are shown for the NO($A^2\Sigma^+$)–Xe PES whose calculation included quadruple excitations.

Figure 5 shows the isotropic parts of the PESs along with the intermolecular potentials used in reference [17] to study the structural relaxation of NO-doped Xe matrices upon photoexcitation of the impurity. In panel a, it can be noticed that both potentials have the same asymptotic behavior because the curves overlap for short and long distances; only in the well part is there a mismatch. In previous references [17,41] where the dynamics of NO-doped Ar and Kr crystals has been addressed, results indicate that the well region is not relevant for the dynamics. In those works, the authors used a Born–Mayer potential instead of a Lennard-Jones form to model the interactions in the excited state, and the results for the dynamics were the same. Only a match of the curves in the Franck–Condon region (repulsive barrier) need be satisfied. The Franck–Condon region is represented by a dotted line that passes through both panels in Figure 5. The isotropic parts of the Xe–NO($A^2\Sigma^+$) PES are represented along with the semiempirical Xe–NO($A^2\Sigma^+$) isotropic potential fitted to the spectroscopic results in reference [17] in panel b. It can

be noticed that the isotropic part of the PES whose calculation included corrections for quadruple excitation meets with the reported potential in reference [17] in the Franck–Condon region while the other potential (without corrections) meets outside, just before the dotted line. This fact is very important for simulating the experimental results for the absorption peak and Stokes shift. The latter quantity indicates the energy released to the lattice in the absorption–emission process.

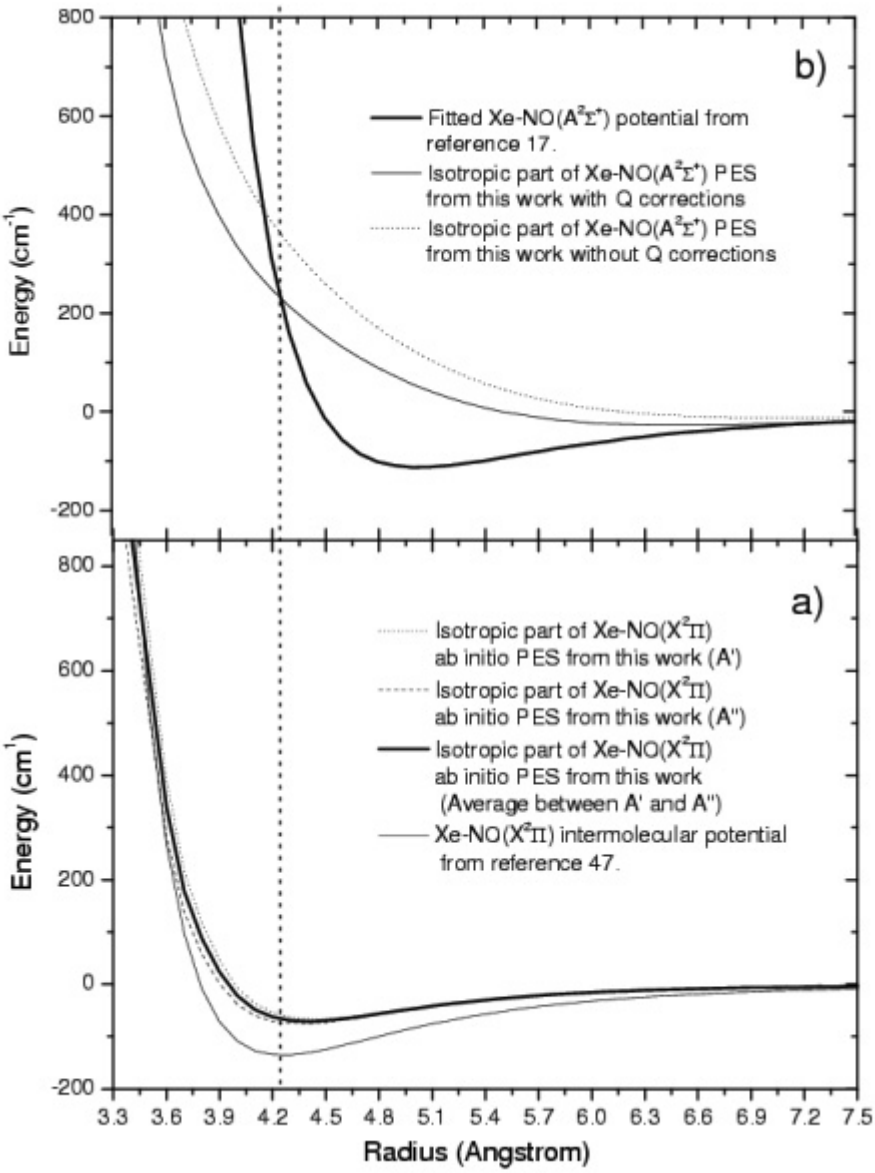

Fig. 5. Curves for the isotropic parts of the NO($X^2\Pi$)–Xe (panel a) and NO($A^2\Sigma^+$)–Xe (panel b) PESs compared with semiempirical isotropic potentials from the literature. The dotted line indicates the Franck–Condon region.

Table 1 gives a comparison among intermolecular potentials for NO–RG complexes in the ground ($X^2\Pi$) and excited ($A^2\Sigma^+$) states. In the case of the ground state, it can be noticed that the NO($X^2\Pi$)–Xe PES shows some differences when compared with the homologous PESs. This PES shows only a T-shape well at 4.1 Å ($\alpha = 83°$) with a depth of –85 cm^{-1} while the rest show two linear wells. The distance of the linear wells from the NO molecule slightly increases and the wells become deeper when the NO($X^2\Pi$)–Ar PES [63] is compared with the NO($X^2\Pi$)–Kr PES [49] in the ground state. In the excited state, the wells are less deep and located at longer distances when

compared with homologous wells in the ground state. For the NO($A^2\Sigma^+$)–Ne PES [64,65], there is only a very shallow linear well with a depth of –3.0 cm^{-1}. However, the NO($A^2\Sigma^+$)–Kr PES [49] shows two linear wells and one T-shape, with depths of –14 cm^{-1}, –10 cm^{-1} and –9 cm^{-1}, respectively. The NO($A^2\Sigma^+$)–Xe PES shows two linear wells, which as expected are deeper when compared with the well depth of the remaining systems because the Xe atom has more electrons affecting the Rydberg state.

Table 1. Comparison among intermolecular potentials for NO–RG complexes in the ground ($X^2\Pi$) and excited ($A^2\Sigma^+$) states. The variables *R* and α indicate the position of the well and *E* the depth. For the ground state, the average PESs are shown, and the excited states include corrections for quadruple excitations, except for NO($A^2\Sigma^+$)–Kr PES.

	NO($X^2\Pi$)-Ar			NO($X^2\Pi$)-Kr			NO($X^2\Pi$)-Xe		
Well	**R(A)**	**α(º)**	**E(cm^{-1})**	**R(A)**	**α(º)**	**E(cm^{-1})**	**R(A)**	**α(º)**	**E(cm^{-1})**
Linear 1	4.22	0	-90	4.4	0	-134			
Linear 2	3.98	180	-90	4.2	180	-128			
T-shape	3.58	93	-115	3.8	95	-145	4.1	83	-85
	NO($A^2\Sigma^+$)-Ne			NO($A^2\Sigma^+$)-Kr			NO($A^2\Sigma^+$)-Xe		
Well	**R(A)**	**α(º)**	**E(cm^{-1})**	**R(A)**	**α(º)**	**E(cm^{-1})**	**R(A)**	**α(º)**	**E(cm^{-1})**
Linear 1	6.5	0	- 3.0	6.0	0	-14	4.90	0	-64
Linear 2				6.6	180	-10	6.24	180	-40
T-shape				7.4	115	-9			

4. Conclusions

PESs for Xe–NO($X^2\Pi$) and Xe–NO($A^2\Sigma^+$) complexes have been presented. The PESs A′ and A″ were calculated for the ground state. Both A′ and A″ show an attractive part characterized by wells with energies ranging from –70 to –100 cm^{-1} and located at distances between 4 and 4.7 Å. In the excited state, two PESs are presented, namely, with or without inclusion of corrections for quadruple excitations in the calculations. For the first case, wells are almost twice as deep and located at slightly shorter distances relative to the second case. There is a noticeable change in the attractive part when quadruple excitation corrections are considered. A comparison among intermolecular potentials for NO–RG complexes in the ground ($X^2\Pi$) and excited ($A^2\Sigma^+$) states showed that the NO($X^2\Pi$)–Xe PES produces some differences when compared with the tendency in the homologous PESs. In the excited states, wells for the NO($A^2\Sigma^+$)–Xe PES are deeper (–64 and –40 cm^{-1}) than wells for the NO($A^2\Sigma^+$)–Ne (–3.5 cm^{-1}) and NO($A^2\Sigma^+$)–Kr (–13.6, –10.1 and –8.5 cm^{-1}) PESs. The Xe–NO PESs presented in this work will allow more complete simulations of structural relaxation of NO-doped Xe systems upon photoexcitation of the NO impurity. These PESs are also expected to be valuable for dynamic studies involving, in general, the Xe–NO triatomic system.

Acknowledgments

This work has been supported by a Grant-in-aid for The 21st Century COE Program for "Chemistry Innovation" from the Ministry of Education, Culture, Sports, Science and Technology of Japan.

References

* Corresponding authors: juanccastro2007@yahoo.com, yamasita@chemsys.t.u-tokyo.ac.jp

[1] V. Chandrasekharan, M. Chergui, B. Silvi and R. D. Etters, J. Phys. Chem. **91**, 1623 (1987).
[2] F. Legay, N. Legay - Sommaire, A. Tramer, M. Chergui and N. Schwentner, J. Phys. Chem. **92**, 261 (1988).
[3] M. Chergui and N. Schwentner, J. Chem. Phys. **91**, 5993 (1989).
[4] A. I. Katz; V.A. Apkarian, Phys. Chem. **94**, 6671 (1990).
[5] R. Schriever, M. Chergui and N. Schwentner, J. Phys. Chem. **95**, 6124 (1991).
[6] Kenneth Haug and Horia Metiu, J. Chem. Phys. **95**, 5670 (1991).

[7] F.Carnovale, J. Barrie, and R.G. Rothwell, J. Chem. Phys. **95**, 1473 (1991).
[8] H. Kunttu; J. Seetula; M. Rasanen; V.A. Apkarian, J. Chem. Phys. **96**, 5630 (1992).
[9] G. J. Hoffman; E. Sekreta; V.A. Apkarian, Chem. Phys. Lett. **191**, 401 (1992).
[10] W.G. Lawrence; V.A. Apkarian, J. Chem. Phys. **97**, 2229 (1992).
[11] W.G. Lawrence; V.A. Apkarian, J. Chem. Phys. **97**, 6199 (1992).
[12] W.G. Lawrence; V.A.Apkarian, J. Chem. Phys. **101**, 1820 (1994).
[13] A.V. Danilychev; V.A.Apkarian, J. Chem. Phys. **100**, 5556 (1994).
[14] J. Helbing, M. Chergui and A. Haydar, J. Chem. Phys. **113**, 3621 (2000).
[15] J. Helbing and M. Chergui, J. Chem. Phys. **94**, 611 (2001).
[16] R. Alimi; V. A. Apkarian; R. Gerber, J. Chem. Phys. **98**, 331 (1993).
[17] J. C. Castro-Palacios, L. Velázquez-Abad, G. Rojas-Lorenzo, J. Rubayo-Soneira, J. Mol. Struct. (THEOCHEM) **730** (2005) 255.
[18] D. M. Leitner, J. D. Doll, and M. Robert, J. Chem. Phys. **94**, 6644 (1991).
[19] P. Scheier, G. Walder, A. Stamatovic, and T.D. Märk, J. Chem. Phys. **90**, 4091 (1989).
[20] Daniel H. Robertson, Franklin B. Brown, and I. Michael Navon, J. Chem. Phys. **90**, 3221 (1989).
[21] J.Sarnthein, A.Pasquarello, R.Car, Phys. Rev. Lett. **74**, 4682 (1995); J.Sarnthein, A.Pasquarello, R.Car, Phys. Rev. B **52**, 12690 (1995); A.Pasquarello, J.Sarnthein, , R.Car, Phys. Rev. B **57**, 14133 (1998); M. Boero, A. Pasquarello, J.Sarnthein, R. Car, Phys. Rev. Lett. **78**, 887 (1997).
[22] R. Car, M. Parinello, Phys. Rev. Lett. **55**, 2471 (1985).
[23] N. Schwentner, E. E. Koch, J. Jortner, Electronic Excitation in Condensed Rare Gas Solids, Springer, Berlin, 1985.
[24] N. Schwentner, V. A. Apkarian, Chem. Rev. **99** (1999) 1481.
[25] M. Chergui, N. Schwentner, V. Chandrasekharan, J. Chem. Phys. **89** (1988) 1277.
[26] I. Ya. Fugol, Adv. in Physics **37** (1978) 1.
[27] F. Vigliotti, M. Chergui, M. Dickgiesser, N. Schwentner, Faraday Discuss. **108** (1997) 139.
[28] J. Goodman, L. E. Brus, J. Chem. Phys. **67** (1977) 933; **69** (1978) 4083.
[29] M. T. Portella-Oberli, C. Jeannin, M. Chergui, Chem. Phys. Lett. **259** (1996) 475.
[30] C. Jeannin, M. T. Portella-Orbeli, F. Vigliotti, M. Chergui, Chem. Phys. Lett. **279** (1997) 65.
[31] M. Chergui, N. Schwentner, W. Böhmer, J. Chem. Phys. **85** (1986) 2472.
[32] L. Bonacina, P. Larrégaray, F. van Mourik, M. Chergui, Phys. Rev. Lett. **95** (2005) 015301.
[33] L. Bonacina, P. Larrégaray, F. van Mourik, M. Chergui, J. Chem. Phys. **125** (2006) 054507.
[34] R. Zadoyan, Z. Li, C. C. Martens, V. A. Apkarian, J. Chem. Phys. **101** (1994) 6648; Z. Li, R. Zadoyan, V. A. Apkarian, C. C. Martens, J. Phys. Chem. **99** (1995) 7435.
[35] Z. Li, J. Y. Fang, C. C. Martens, J. Chem. Phys.**104** (1996) 6919.
[36] A. Goldberg, J. Jortner, J. Chem. Phys. **107** (1997) 8994.
[37] S. Cui, R. E. Johnson, P. Cummings, Surf. Sci. **207** (1988) 186.
[38] A. Borrman, C. C. Martens, J. Chem. Phys. **102** (1995) 1905.
[39] J. Jortner, in Femtochemistry, Ultrafast Chemical and Physical Processes in Molecular Systems, edited by M. Chergui, World Scientific, Singapore, 1996, p. 15.
[40] J. Wörmer, R. Karabach, M. Joppien, T. Möller, J. Chem. Phys. **104** (1996) 8269; O. Bjorneholm, F. Federmann, F. Fösing, T. Möller Phys. Rev. Lett. **74** (1995) 3017; O. Bjorneholm, F. Federmann, F. Fösing, T. Möller , S. Stampfli, J. Chem. Phys. **104** (1996) 1876; M. Lengen, M. Joppien, R. von Pietrowski, T. Möller, Chem. Phys. Letter **229** (1994) 362.
[41] S. Jimenez, M. Chergui, G. Rojas-Lorenzo, J. Rubayo-Soneira, J. Chem. Phys. **114** (2001) 5264.
[42] F. Vigliotti, L. Bonacina, M. Chergui, G. Rojas-Lorenzo, J. Rubayo-Soneira, Chem. Phys. Lett. **362**, 31 (2002).
[43] G. Rojas-Lorenzo, J. Rubayo-Soneira, F. Vigliotti, M. Chergui, Phys. Rev. B **67** (2003) 115119.
[44] G. Rojas-Lorenzo, J. Rubayo-Soneira, S. Fernández-Alberti, M. Chergui, J. Phys. Chem. A **107** (2003) 8225.
[45] J. C. Castro-Palacios, L. Velázquez-Abad, G. Rojas-Lorenzo, J. Rubayo-Soneira, Eur. Phys. J. D **25** (2003) 149.
[46] J. Rubayo-Soneira, J. C. Castro-Palacios, G. Rojas-Lorenzo, Phys. Stat. Solidi B **242** (2005) 1747.
[47] H. H. W. Thuis, S. Stolte, J. Reuse, J. J. H. van den Biessen, C. J. N. van den Meidenberg, Chem. Phys. **52** (1980) 211.
[48] A. García-Vela, J. Rubayo-Soneira, G. Delgado Barrio, P. Villarreal, J. Chem. Phys. **104** (1996) 8405.
[49] J. C. Castro-Palacios, J. Rubayo-Soneira, K. Ishii, K. Yamashita, J. Chem. Phys. **126** (2007) 134315.
[50] J. C. Castro-Palacios, L. Velázquez, J. Rubayo-Soneira, A. Lombardi, V. Aquilanti, J. Chem. Phys. **126** (2007) 174701.
[51] J. C. Castro-Palacios, J. Rubayo-Soneira, A. Lombardi, V. Aquilanti, Int J Quantum Chem, **108**, 1821 (2008).
[52] H.-J. Werner, P. J. Knowles, J. Chem. Phys. **82** (1985) 5053.
[53] H.-J. Werner, P. J. Knowles, J. Chem. Phys. **89** (1988) 5803.
[54] T. H. Dunning, Jr., J. Chem. Phys. **90** (1989) 1007.
[55] R. A. Kendall, T. H. Dunning, Jr., R. J. Harrison, J. Chem. Phys. **96** (1992) 6769.
[56] MOLPRO is a package of ab initio programs written by H.-J. Werner, P.J. Knowles, with contributions from R.D. Amos, A. Bernhardsson, A. Berning, P. Celani, D.L. Cooper, M.J.O. Deegan, A.J. Dobbyn, F. Eckert, C. Hampel, G. Hetzer, T. Korona, R. Lindh, A.W. Lloyd, S.J. McNicholas, F.R. Manby, W. Meyer, M.E. Mura, A. Nicklass, P. Palmieri, R. Pitzer, G. Rauhut, M. Schütz, H. Stoll, A. b J. Stone, R. Tarroni, T. Thorsteinsson.
[57] G. Chalasiński, M. Szczęśniak, Chem. Rev. **100** (2000) 4227.
[58] J. H. van Lenthe, T. van Dam, F.B. van Duijneveldt.; L.M. J. Kroon-Batenburg, Faraday Symp. Soc. **19** (1984) 1.
[59] M.H.Alexander, J.Chem.Phys. **108** (1998) 4467.
[60] K. Stark, H.J.Werner, J. Chem. Phys. **104** (1996) 6515.
[61] M.S. Topaler, D.G.Truhlar; X.Y.Chang, P. Piecuch, J.C. Polanyi, J.Chem.Phys. **108** (1998) 5349.
[62] A.L.Kaledin, M.C. Heaven, W.G. Lawrence, Q. Cui, J.E. Stevens, K. Morokuma J.Chem Phys. **108** (1998) 2771.
[63] Y. Sumiyoshi, Y. Endo. J. Chem. Phys. **127** (2007) 184309.
[64] P. Pajon-Suárez, G. Rojas-Lorenzo, J. Rubayo-Soneira, R. Hernández-Lamoneda. Chem. Phys. Lett. **421** (2006) 389.

[65] V. L. Ayles, R. J. Plowright, M. J. Watkins, T. G. Wright, J. Klos, M. Alexander, P. Pajón-Suárez, J. Rubayo-Soneira and R. Hernández-Lamoneda. Chem.Phy. Lett. **441** (2007) 181.
[66] J. Kłos, M. H. Alexander, R. Hernández-Lamoneda and T G. Wright, J. Chem. Phys. **129** (2008) 244303.
[67] P.J. Knowles, C. Hampel, H.-J. Werner, J. Chem. Phys. **99** (1993) 5219.